DYNAMIC CHARACTERISTICS OF A TWO-SPOOL GAS TURBINE HELICOPTER ENGINE

By

E. J. Gunter, Professor*
D. F. Li, Associate Senior Research Engineer**
L. E. Barrett, Research Assistant Professor*

*Department of Mechanical and Aerospace Engineering
University of Virginia
Charlottesville, Virginia

**General Motors Research Laboratories
Warren, Michigan

ABSTRACT

This paper presents a dynamic analysis of a two-spool gas turbine helicopter engine incorporating intershaft rolling element bearings between the gas generator and power turbine rotors. The analysis includes the nonlinear effects of a squeeze film bearing incorporated on the gas generator rotor. The analysis includes critical speeds and forced response of the system and indicates that substantial dynamic loads may be imposed on the intershaft bearings and main bearing supports with an improperly designed squeeze film bearing. A comparison of theoretical and experimental gas generator rotor response is presented illustrating the nonlinear characteristics of the squeeze film bearing. It was found that large intershaft bearing forces may occur even though the engine is not operating at a resonant condition.

INTRODUCTION

The requirement of high specific power output for gas turbine aircraft engines has resulted in highly flexible rotor designs. These rotors typically operate above several critical speeds. The use of rolling element bearings, with low inherent damping, makes it difficult to reduce vibrational amplitudes and dynamic loads transmitted to the rotor supporting structure. Operation over a wide range of speed and power levels aggravates the dynamic problems, and under some conditions, i.e. locked rotor starts, a bowed rotor may result due to nonuniform thermal distributions.

The low levels of rolling element bearing damping and large strain energy levels in modern designs necessitate the use of squeeze film bearings to provide adequate damping to maintain low amplitude vibration levels and to reduce the dynamic loads exerted upon the bearings and rotor support structures. The number and location of squeeze film bearings is dictated by

On the basis of the simplified linear theory some damper characteristics of direct interest to the designer can be calculated. The more important are the transmissibility, the effective damping and the effective stiffness. The definitions and formulas are given in the references. Examples of the effective damping and stiffness as a function of speed are given in Figs. 5 & 6. The damping appears again to be sensitive to the viscosity of the oil. Both figures have limited validity at higher speeds because of the linearization.

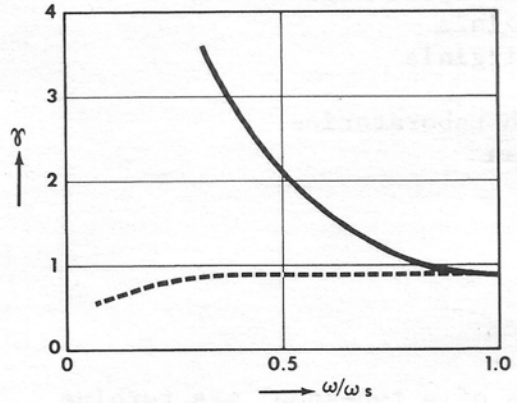

Fig. 5

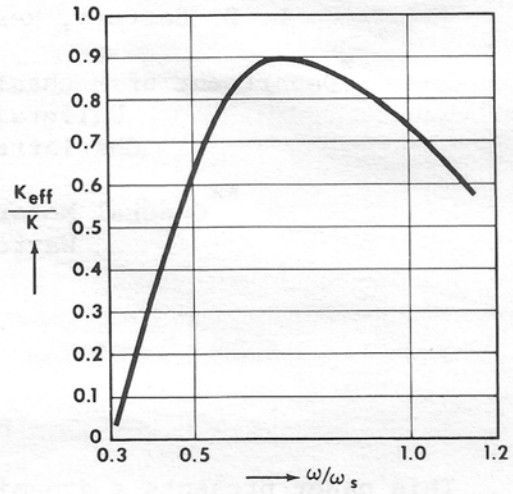

Fig. 6

CONCLUSION

The rig has performed satisfactorily allowing the measurement of all oil-film parameters over a wide speed range. The rig is especially useful for investigations of transient response phenomena.

The linearized theory appears adequate for the range of small eccentricities at which dampers operate in practice.

REFERENCES

1. Botman, M., "Experiments on Oil-Film Dampers for Turbomachinery", ASME Journal of Engineering for Power, Vol. 98, No. 3, July 1976, pp. 393-400.

2. Botman, M. and Sharma, R.K., "Experiments on the Transient Response of Oil-Film Dampers", ASME Journal of Engineering for Power, Vol. 100, No.1, Jan. 1978, pp. 30-35.

3. Sharma, R.K. and Botman, M., "An Experimental Study of the Steady-State Response of Oil-Film Dampers", ASME Journal of Mechanical Design, Vol. 100, No. 2, April 1978, pp. 216-221.

the engine configuration and dynamic characteristics (1). In addition, engines may utilize intershaft differential bearings, especially with very flexible rotor designs. The design of squeeze film bearings requires careful attention since an improper design may, in fact, worsen the dynamic response of the system (2).

A schematic of a typical two-spool gas turbine engine used for helicopter application is shown in Fig. 1. The engine consists of an inner core rotor (power turbine), which is supported by main bearings No. 0 and No. 4, located at the shaft extremities. There are two intershaft differential bearings connecting the power turbine to the gas generator rotor. The gas generator rotor consists of a two-stage turbine which drives an axial compressor. The gas generator rotor is supported principally by the Nos. 1, 2, and 3 bearings.

The No. 1 bearing is an elliptical roller bearing mounted in a thermal gradient housing. The No. 2 bearing is a thrust ball bearing mounted in the compressor rear frame, and the No. 3 or aft bearing is a close clearance roller bearing mounted in an oil film damper support near the gas generator turbine. The No. 0 roller bearing is mounted in the power turbine take off and supports the output turbine spline shaft. The No. 4 bearing is located in the exhaust frame and is a thrust ball bearing that carries the weight of the power turbine. The first or forward intershaft bearing is an elliptic differential bearing mounted between the power turbine shaft and the compressor No. 1 bearing. The second or aft intershaft bearing is mounted forward of the No. 3 bearing.

The gas generator rotor speed range is from 10,500 RPM to 18,230 RPM, and the power turbine speed is from 0 to 17,000 RPM. Typical continuous power turbine operating speed is 14,000 RPM.

The analysis presented herein includes both flexible rotors, the effects of the intershaft bearings, and the bearings connecting the rotors to the engine case. The case is considered rigid, although casing flexibility may be an important effect in certain applications.

CRITICAL SPEED ANALYSIS

The preliminary analysis of any rotor-bearing system usually includes the determination of the undamped critical speeds and associated mode shapes of the system. These results provide the basis for refining the system model and anticipating locations where squeeze film bearings may be potentially applied, i.e., locations where significant motion of the squeeze film bearing journal will occur to produce the required damping forces. The critical speed analysis utilized the transfer matrix method (3), (4).

Critical Speeds with Intershaft Bearings

Figures 2-4 illustrate the first three critical speed mode shapes of the two-spool engine of Fig. 1, including the stiffness of the intershaft bearings. For this analysis the gas generator rotor was assumed to be operating at 15,000 RPM and the critical speeds were calculated assuming synchronous motion of the power turbine.

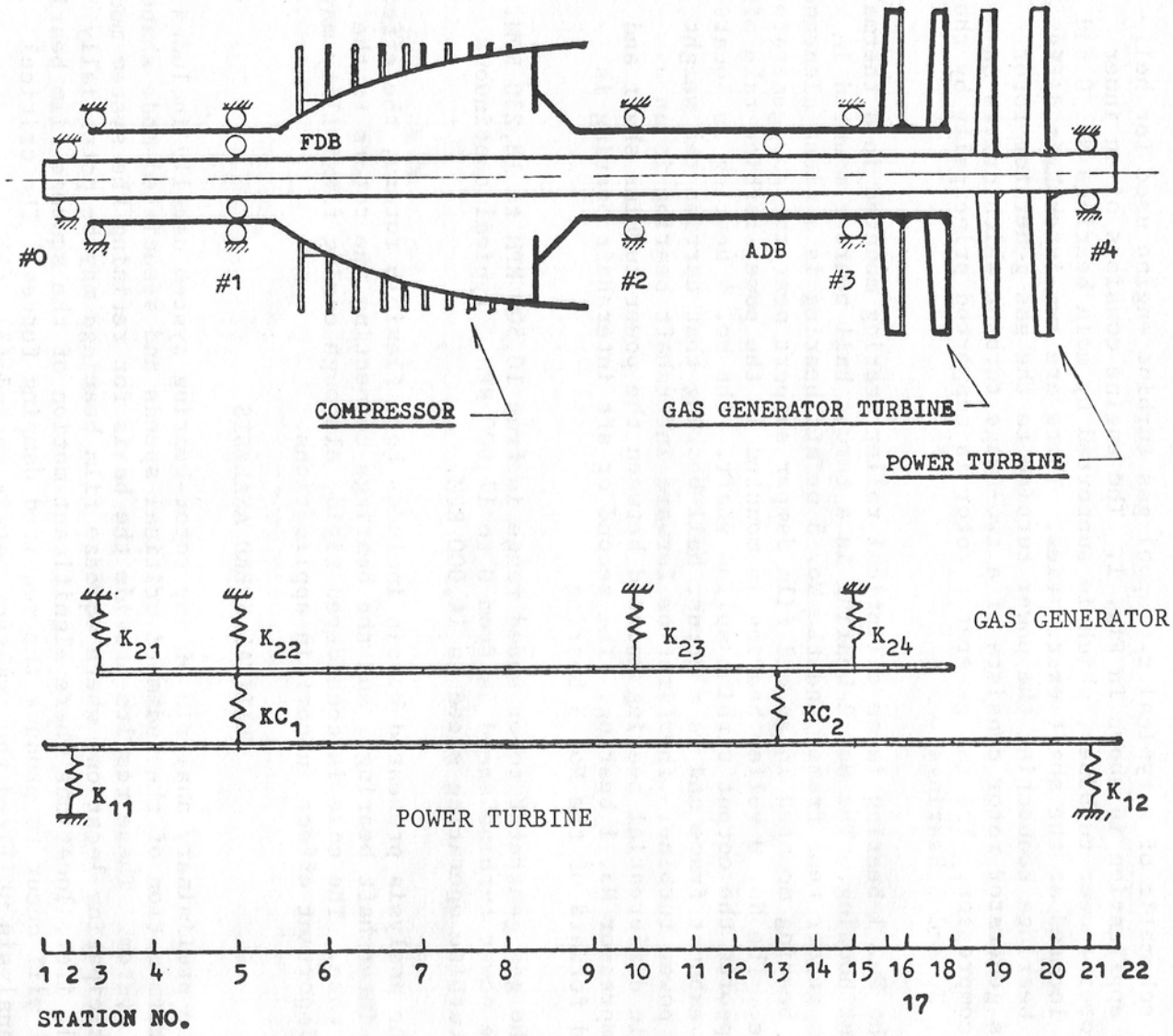

Fig. 1 Schematic of Two-Spool Gas Turbine Helicopter Engine with Computer Model.

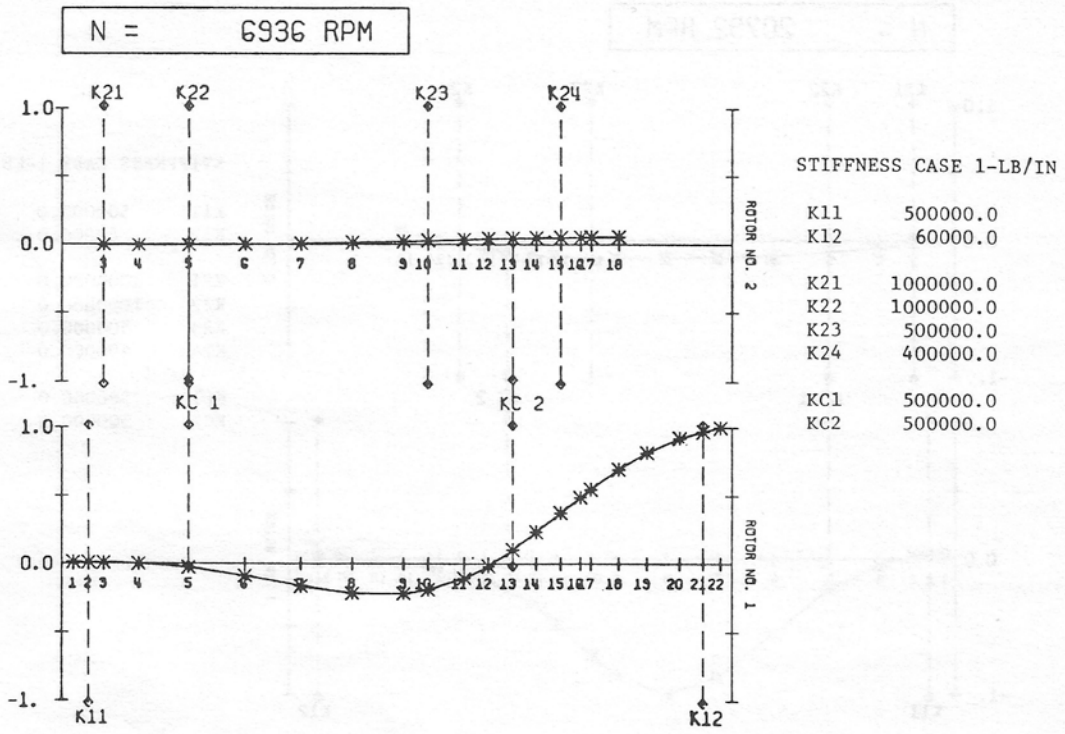

Fig. 2 First Engine Undamped Critical Speed with Aft Intershaft Differential Bearing

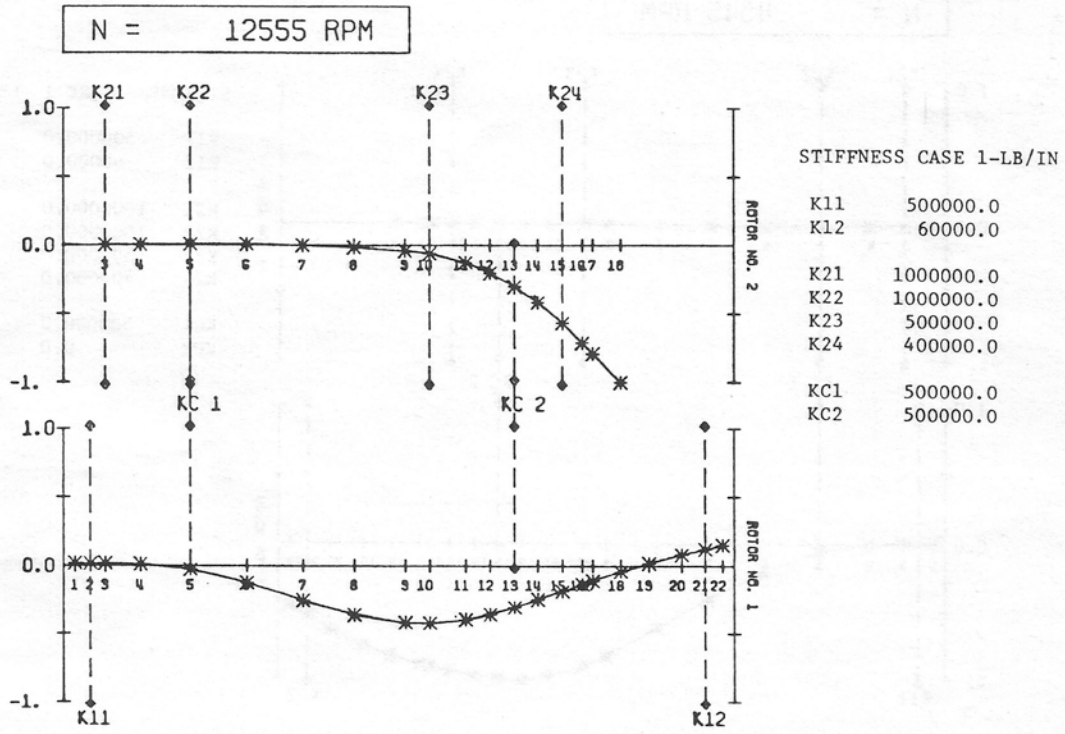

Fig. 3 Second Engine Undamped Critical Speed with Aft Intershaft Differential Bearing

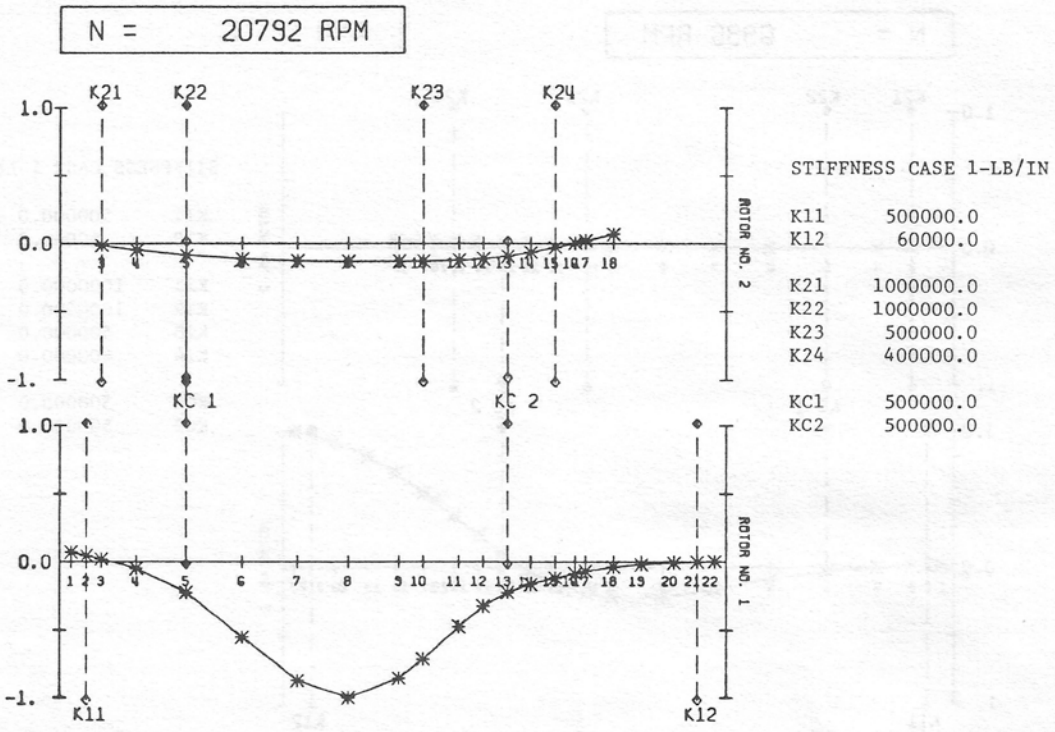

Fig. 4 Third Engine Undamped Critical Speed with Aft Intershaft Differential Bearing

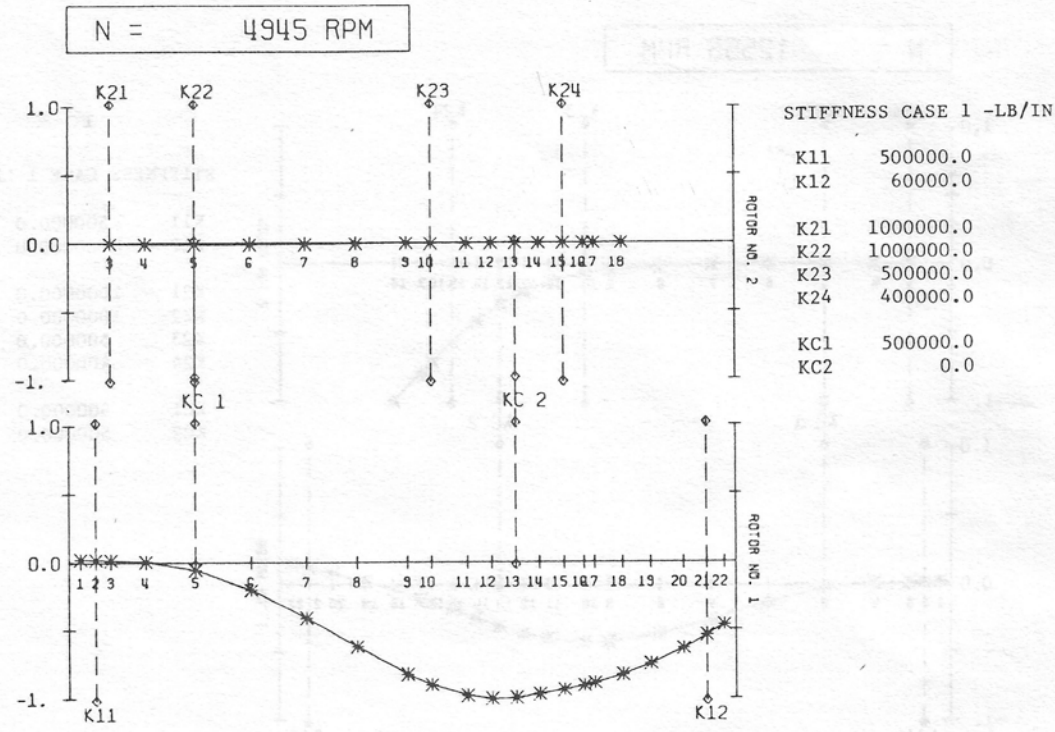

Fig. 5 First Engine Undamped Critical Speed without Aft Intershaft Differential Bearing

Figure 2 shows that the first critical speed at 6,936 RPM is predominantly a bending mode of the power turbine. The largest amplitude occurs at the power turbine location. It can be observed that a squeeze film bearing located at the No. 4 bearing (K12) would be extremely effective in damping out this particular mode.

A slight deflection of the gas generator rotor is observed for this mode due to the forces transmitted through the aft intershaft differential bearing (KC2). A squeeze film bearing employed at the gas generator No. 3 bearing support (K24) will not effectively suppress this mode. Since there is little motion at the aft intershaft differential bearing (KC2) at this mode, unbalance at the gas generator location should cause relatively little excitation of the power turbine first mode. This mode will be primarily influenced by unbalance at the power turbine stages. If the power turbine unbalance is excessive, then tip rubs of the power turbine blades could occur.

Figure 3 illustrates the second system critical speed mode shape. This mode at 12,555 RPM represents the first gas generator mode with the motion primarily occurring in the gas generator rotor turbine section. The aft intershaft differential bearing (KC2) connecting the gas generator and the power turbine causes a considerable deflection of the power turbine shaft. It appears possible that should the power turbine shaft become thermally bowed, it may excite this mode. Substantial loads would be transmitted through the aft intershaft differential bearing. Since the motion at the No. 4 bearing (K12) is small, a squeeze film bearing at this location would be relatively ineffective in suppressing the power turbine motion due to excitation from the gas generator. A squeeze film bearing located behind the No. 3 bearing (K24) should be quite effective in suppressing this mode if properly designed. The actual bearing loads transmitted through the various bearings will be examined in a subsequent section.

The third system critical speed of the gas turbine is predicted to be 20,792 RPM. The mode shape is shown in Fig. 4. This critical is above the operating speed range of both the gas generator rotor or the turbine. One interesting observation from this mode is that the aft intershaft differential bearing causes considerable deflection of the power turbine shaft. This mode would be particularly excited if there were a residual bow in the power turbine shaft. Such a bow might be produced by thermal gradients. Although this critical speed is predicted to be over 20,000 RPM, large differential bearing forces may be developed at speeds below this critical speed due to the shaft deflection caused by the intershaft differential bearing. The relatively small motion that occurs at the gas generator No. 3 bearing suggests that a squeeze film bearing there would be relatively ineffective.

Critical Speeds without Aft Intershaft Differential Bearing

Under certain operating conditions, such as a locked power turbine rotor start, excessive wear and degradation have occurred in the aft intershaft differential bearing. The critical speeds and mode shapes for the system were also calculated assuming negligible aft intershaft differential bearing stiffness. The first critical speed of the system without the aft

intershaft is approximately 4,945 RPM, a reduction of nearly 2,000 RPM. Figure 5 shows that this mode shape has changed considerably from the original first critical speed as shown in Fig. 2. The highest amplitude of motion with this mode does not occur at the power turbine but near the aft intershaft differential bearing and the internal seals. It appears likely that this mode could be excited by a bow in the power turbine rotor. The relative motion at the forward intershaft differential bearing is small and there is little motion of gas generator rotor as this is primarily a power turbine rotor mode.

The second mode without the aft intershaft differential bearing is shown in Fig. 6. The critical speed for this mode is approximately 11,500 RPM. This mode is also primarily a power turbine rotor mode and is well within the normal operating speed range of the power turbine rotor and would be easily excited by power turbine unbalance or bow of the power turbine rotor. Sustained operation at this mode could result in the power turbine rubbing on the gas generator rotor. Experimental testing of this engine configuration without the aft intershaft differential bearing showed evidence of rubbing at the center of the power turbine rotor. It is evident from Figs. 5 and 6 that a squeeze film bearing mounted at the gas generator rotor No. 3 bearing support would be ineffective in suppressing either of the first two engine modes with a failed or eliminated aft intershaft differential bearing.

The third engine critical speed is approximately 12,500 RPM, and the mode shape is shown in Fig. 7. This mode is essentially the same as the second mode with full aft intershaft differential bearing stiffness and is primarily a gas generator rotor mode. The relatively large motion that occurs at the gas generator No. 3 bearing implies that a squeeze film bearing at this location would be effective in suppressing this mode.

Because the rotors in this engine are quite flexible, the intershaft differential bearings are essential components to ensure that rubbing between the two rotors does not occur. The aft intershaft differential bearing plays an important role in determining the second power turbine rotor critical speed. Loss of stiffness in this bearing results in a reduction of the power turbine rotor second critical speed which then occurs within the normal engine operating speed range. It is also apparent from the critical speed mode shapes that a single squeeze film bearing may not provide adequate damping capability for all engine modes within the engine operating speed range.

GAS TURBINE ENGINE UNBALANCE RESPONSE

Although the undamped critical speeds and mode shapes presented in the previous secion provide useful design information, they do not provide quantitative information on the vibration amplitudes, bearing forces and effects of damping with unbalance forces acting on the system. This section describes the results of an unbalance response analysis of the engine, including both linear and nonlinear squeeze film bearing forces. The transfer matrix method was also used to generate the results (4), (5).

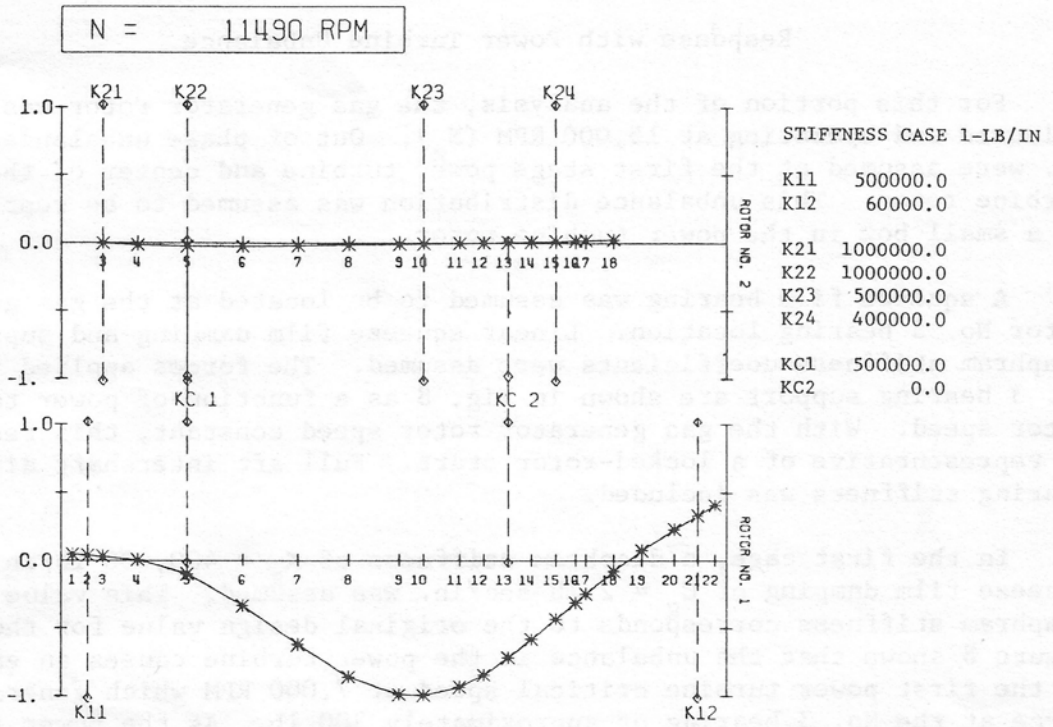

Fig. 6 Second Engine Undamped Critical Speed without Aft Intershaft Differential Bearing

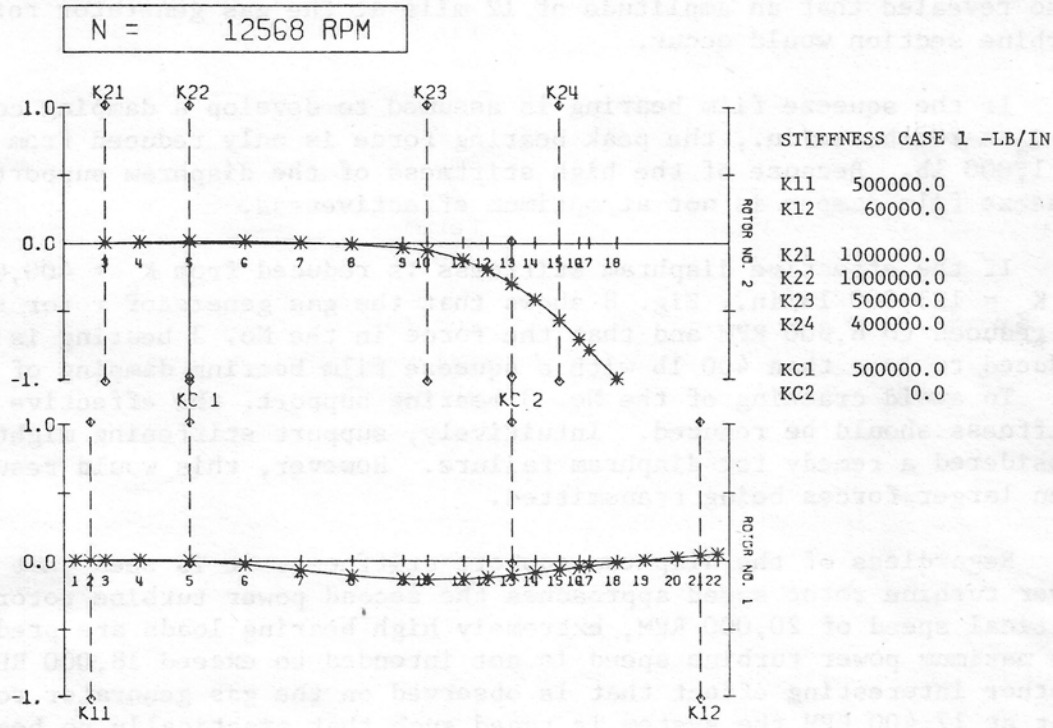

Fig. 7 Third Engine Undamped Critical Speed without Aft Intershaft Differential Bearing

Response with Power Turbine Unbalance

For this portion of the analysis, the gas generator rotor was considered balanced and operating at 15,000 RPM (N_g). Out of phase unbalances of 10 gm-in. were assumed at the first stage power turbine and center of the power turbine rotor. This unbalance distribution was assumed to be representative of a small bow in the power turbine rotor.

A squeeze film bearing was assumed to be located at the gas generator rotor No. 3 bearing location. Linear squeeze film damping and support diaphram stiffness coefficients were assumed. The forces applied to the No. 3 bearing support are shown in Fig. 8 as a function of power turbine rotor speed. With the gas generator rotor speed constant, this response is representative of a locked-rotor start. Full aft intershaft differential bearing stiffness was included.

In the first case, a diaphram stiffness of K_g = 400,000 lb/in. and squeeze film damping of C_g = 2 lb-sec/in. was assumed. This value of diaphram stiffness corresponds to the original design value for the engine. Figure 8 shows that the unbalance in the power turbine causes an excitation of the first power turbine critical speed at 7,000 RPM which generates a force at the No. 3 bearing of approximately 300 lb. As the power turbine speed is increased, a very large resonance peak occurs at 12,000 RPM, resulting in a peak force of 2,650 lb. In the actual testing of this engine, cracking of the gas generator diaphram has occurred along with seal rubs on the gas generator turbine. Both of these effects could be initiated by a bowed power turbine shaft during a locked rotor start since the analysis also revealed that an amplitude of 12 mils at the gas generator rotor turbine section would occur.

If the squeeze film bearing is assumed to develop a damping coefficient of C_g = 20 lb-sec/in., the peak bearing force is only reduced from 2,650 lb to 1,000 lb. Because of the high stiffness of the diaphram support, the squeeze film damper is not at optimum effectiveness.

If the effective diaphram stiffness is reduced from K_g = 400,000 lb/in. to K_g = 123,000 lb/in., Fig. 8 shows that the gas generator rotor resonance is reduced to 8,800 RPM and that the force in the No. 3 bearing is also reduced to less than 400 lb with a squeeze film bearing damping of 20 lb-sec/in. To avoid cracking of the No. 3 bearing support, the effective diaphram stiffness should be reduced. Intuitively, support stiffening might be considered a remedy for diaphram failure. However, this would result in even larger forces being transmitted.

Regardless of the diaphram support stiffness, it is seen that as the power turbine rotor speed approaches the second power turbine rotor critical speed of 20,000 RPM, extremely high bearing loads are predicted. The maximum power turbine speed is not intended to exceed 18,000 RPM. Another interesting effect that is observed on the gas generator rotor is that at 17,400 RPM the system is tuned such that practically no bearing forces are transmitted. Hence, at this speed, even with large power turbine unbalance values, little motion would be observed on the gas generator.

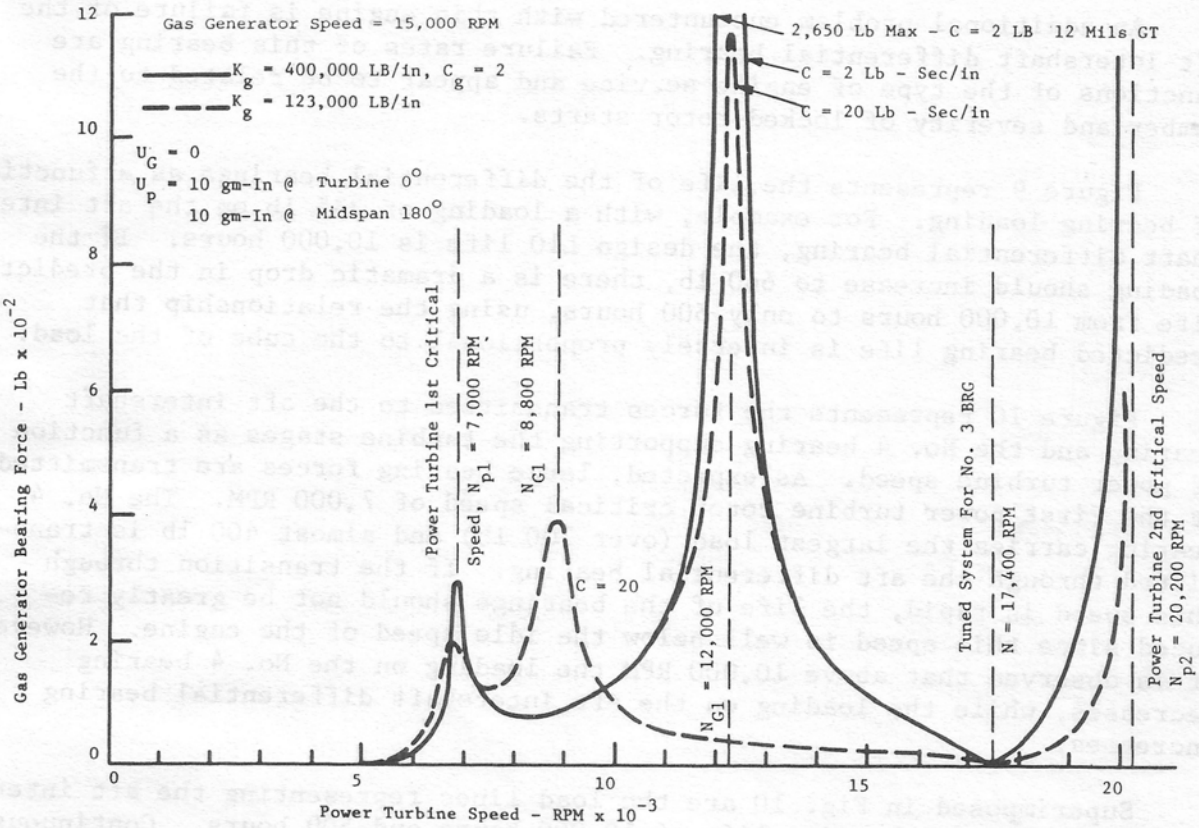

Fig. 8 Forces in No. 3 Bearing Due to Power Turbine Unbalance

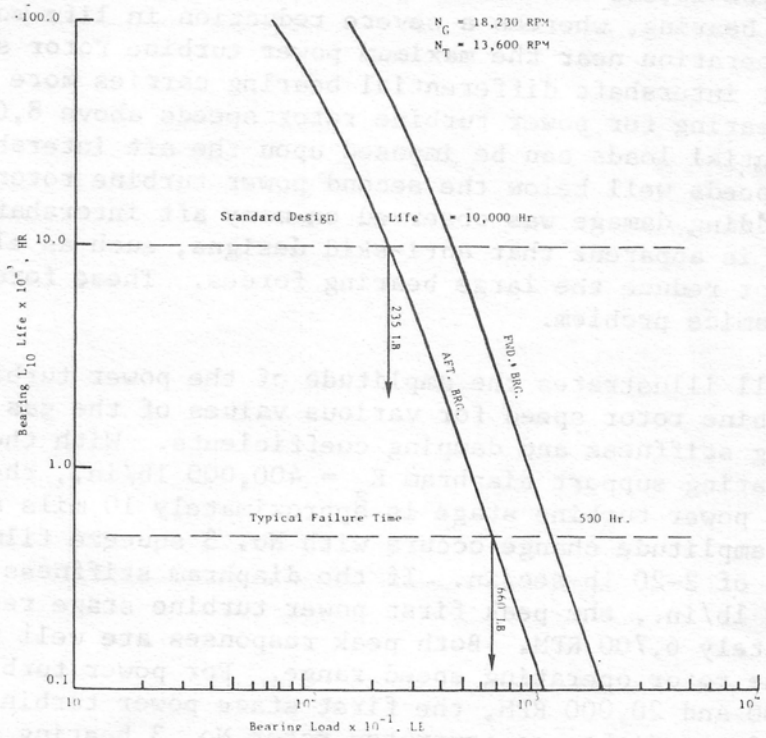

Fig. 9 Intershaft Differential Bearing Life as a Function of Bearing Load

An additional problem encountered with this engine is failure of the aft intershaft differential bearing. Failure rates of this bearing are functions of the type of engine service and appear to be related to the number and severity of locked-rotor starts.

Figure 9 represents the life of the differential bearings as a function of bearing loading. For example, with a loading of 235 lb on the aft intershaft differential bearing, the design L10 life is 10,000 hours. If the loading should increase to 660 lb, there is a dramatic drop in the predicted life from 10,000 hours to only 500 hours, using the relationship that predicted bearing life is inversely proportional to the cube of the load.

Figure 10 represents the forces transmitted to the aft intershaft bearing and the No. 4 bearing supporting the turbine stages as a function of power turbine speed. As expected, large bearing forces are transmitted at the first power turbine rotor critical speed of 7,000 RPM. The No. 4 bearing carries the largest load (over 700 lb) and almost 400 lb is transmitted through the aft differential bearing. If the transition through this speed is rapid, the life of the bearings should not be greatly reduced since this speed is well below the idle speed of the engine. However, it is observed that above 10,000 RPM the loading on the No. 4 bearing decreases, while the loading on the aft intershaft differential bearing increases.

Superimposed in Fig. 10 are the load lines representing the aft intershaft differential bearing life of 10,000 hours and 500 hours. Continuous operation below 14,000 RPM would not reduce the life of the aft intershaft differential bearing, whereas a severe reduction in life would occur with continuous operation near the maximum power turbine rotor speed of 17,400 RPM. The aft intershaft differential bearing carries more load than the main No. 4 bearing for power turbine rotor speeds above 8,000 RPM. Furthermore, substantial loads can be imposed upon the aft intershaft differential bearing at speeds well below the second power turbine rotor critical speed. Although skidding damage was observed on many aft intershaft differential bearings, it is apparent that anti-skid designs, such as elliptical bearings, will not reduce the large bearing forces. These forces are an inherent dynamics problem.

Figure 11 illustrates the amplitude of the power turbine as a function of power turbine rotor speed for various values of the gas generator rotor No. 3 bearing stiffness and damping coefficients. With the stiffness of the No. 3 bearing support diaphram K_g = 400,000 lb/in., the peak amplitude of the first power turbine stage is approximately 10 mils at 7,000 RPM. Very little amplitude change occurs with No. 3 squeeze film bearing damping coefficients of 2-20 lb-sec/in. If the diaphram stiffness is reduced to K_g = 123,000 lb/in., the peak first power turbine stage response is 7 mils at approximately 6,700 RPM. Both peak responses are well below the normal power turbine rotor operating speed range. For power turbine rotor speeds between 8,000 and 20,000 RPM, the first stage power turbine response is low, independent of the gas generator rotor No. 3 bearing stiffness and damping coefficients. A large response also occurs at the second power turbine rotor critical speed (20,200 RPM) and is relatively unaffected by the No. 3 bearing characteristics, as predicted by the critical speed

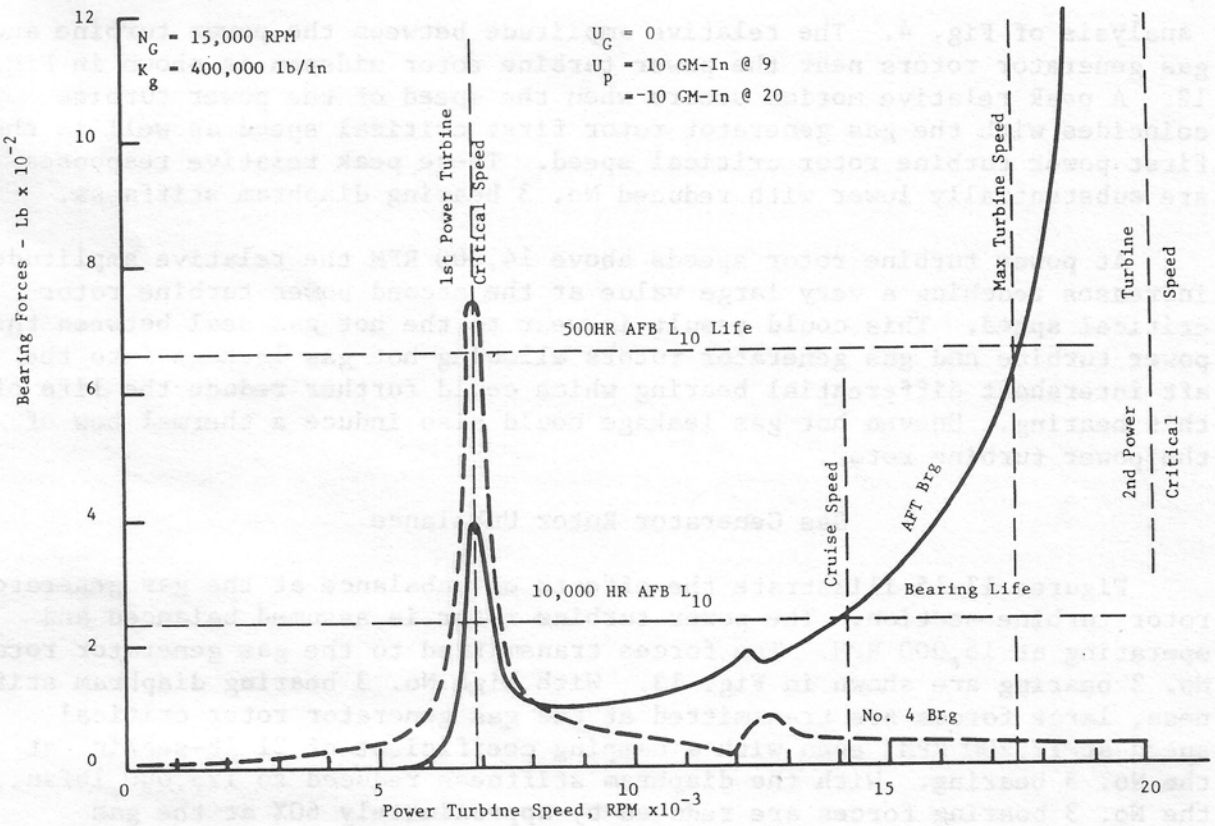

Fig. 10 Aft Intershaft Differential Bearing Load Due to Power Turbine Unbalance

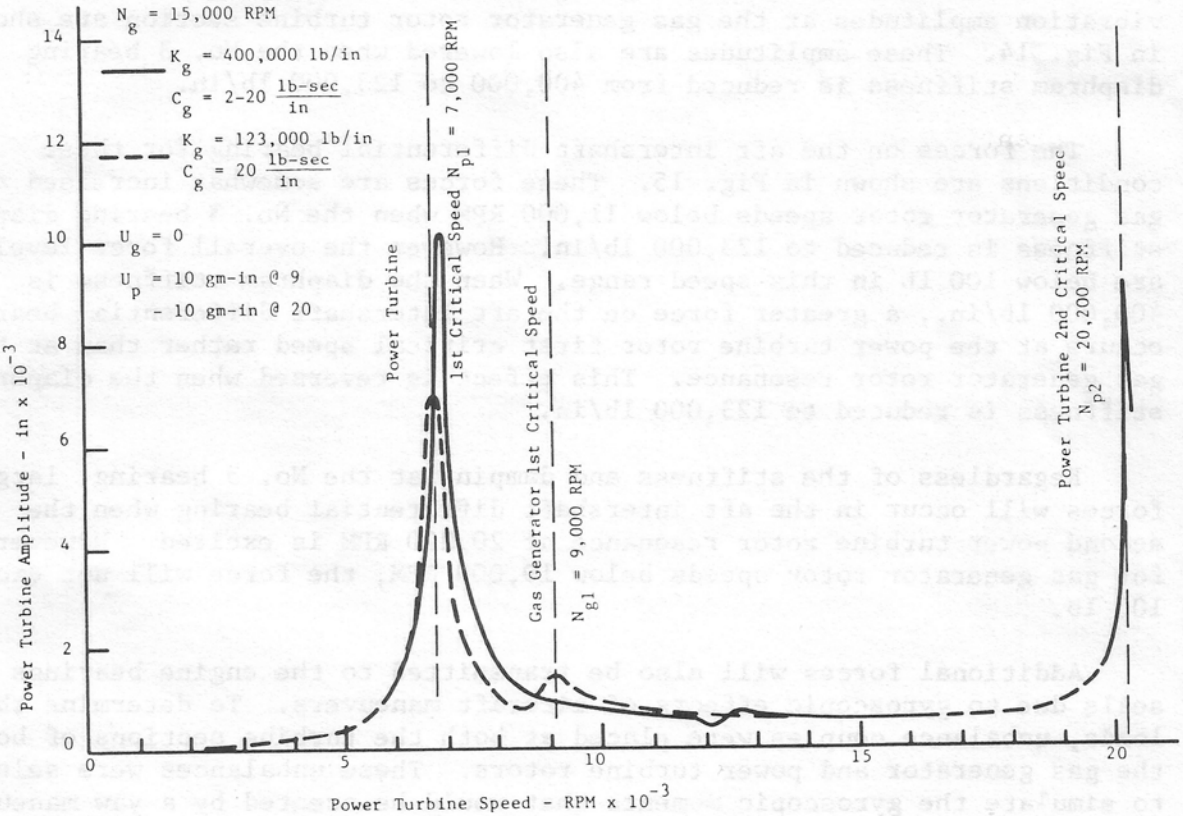

Fig. 11 Power Turbine Amplitude Due to Power Turbine Unbalance

analysis of Fig. 4. The relative amplitude between the power turbine and gas generator rotors near the power turbine rotor midspan is shown in Fig. 12. A peak relative motion occurs when the speed of the power turbine coincides with the gas generator rotor first critical speed as well as the first power turbine rotor critical speed. These peak relative responses are substantially lower with reduced No. 3 bearing diaphram stiffness.

At power turbine rotor speeds above 14,000 RPM the relative amplitude increases reaching a very large value at the second power turbine rotor critical speed. This could result in wear to the hot gas seal between the power turbine and gas generator rotors allowing hot gas leakage into the aft intershaft differential bearing which could further reduce the life of this bearing. Uneven hot gas leakage could also induce a thermal bow of the power turbine rotor.

Gas Generator Rotor Unbalance

Figures 13-15 illustrate the effects of unbalance at the gas generator rotor turbine section. The power turbine rotor is assumed balanced and operating at 15,000 RPM. The forces transmitted to the gas generator rotor No. 3 bearing are shown in Fig. 13. With high No. 3 bearing diaphram stiffness, large forces are transmitted at the gas generator rotor critical speed at 12,200 RPM, even with a damping coefficient of 21 lb-sec/in. at the No. 3 bearing. With the diaphram stiffness reduced to 123,000 lb/in., the No. 3 bearing forces are reduced by approximately 60% at the gas generator rotor resonant speed of 8,600 RPM. Very little excitation of the power turbine rotor occurs with gas generator rotor unbalance. The vibration amplitudes at the gas generator rotor turbine section are shown in Fig. 14. These amplitudes are also lowered when the No. 3 bearing diaphram stiffness is reduced from 400,000 to 123,000 lb/in.

The forces on the aft intershaft differential bearing for these conditions are shown in Fig. 15. These forces are somewhat increased at gas generator rotor speeds below 11,000 RPM when the No. 3 bearing diaphram stiffness is reduced to 123,000 lb/in. However the overall force levels are below 100 lb in this speed range. When the diaphram stiffness is 400,000 lb/in., a greater force on the aft intershaft differential bearing occurs at the power turbine rotor first critical speed rather than at the gas generator rotor resonance. This effect is reversed when the diaphram stiffness is reduced to 123,000 lb/in.

Regardless of the stiffness and damping at the No. 3 bearing, large forces will occur in the aft intershaft differential bearing when the second power turbine rotor resonance at 20,200 RPM is excited. However, for gas generator rotor speeds below 19,000 RPM, the force will not exceed 100 lb.

Additional forces will also be transmitted to the engine bearings and seals due to gyroscopic effects of aircraft maneuvers. To determine these loads, unbalance couples were placed at both the turbine sections of both the gas generator and power turbine rotors. These unbalances were selected to simulate the gyroscopic moments that would be created by a yaw maneuver of 0.2 RPS. The results are summarized in Table 1. The largest forces

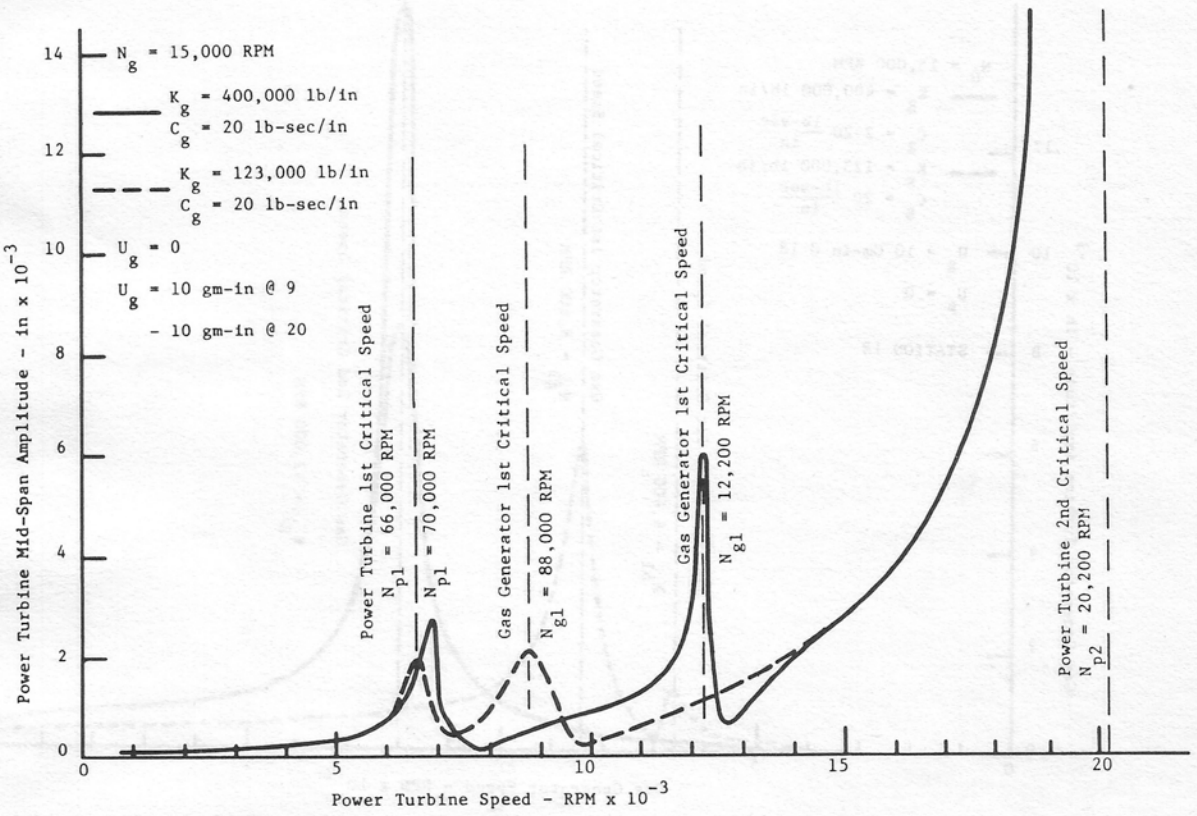

Fig. 12 Power Turbine Midspan Amplitude Due to Power Turbine Unbalance

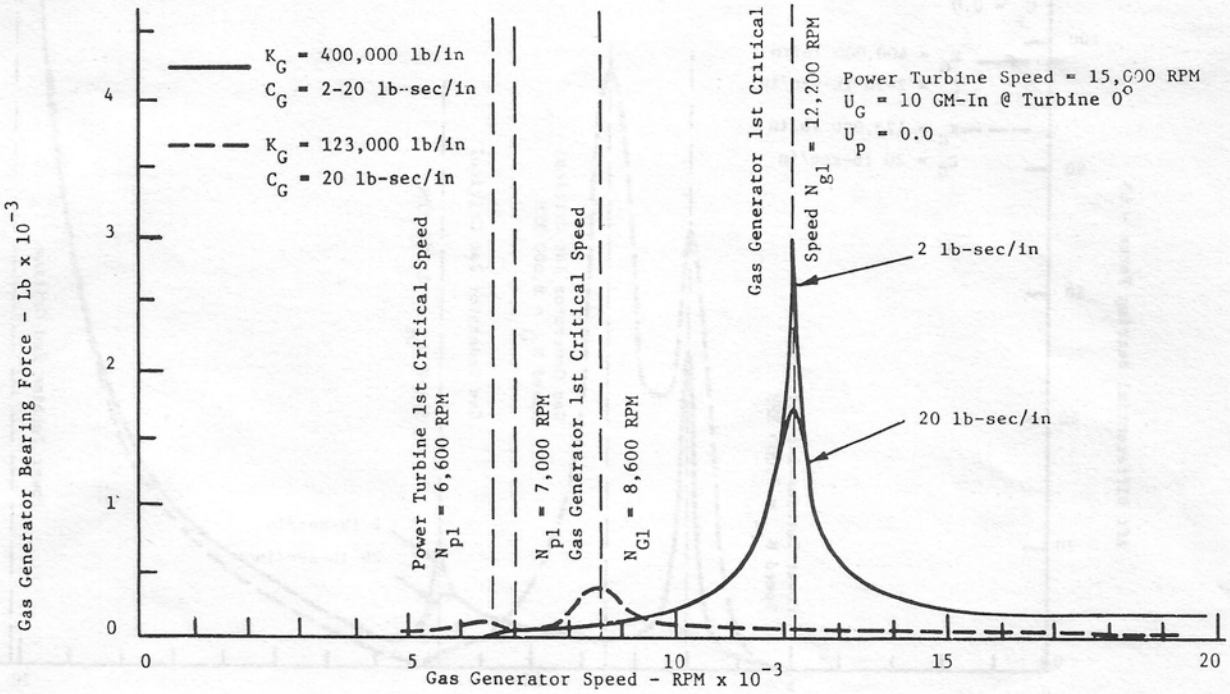

Fig. 13 No. 3 Bearing Forces Due to Gas Generator Turbine Unbalance

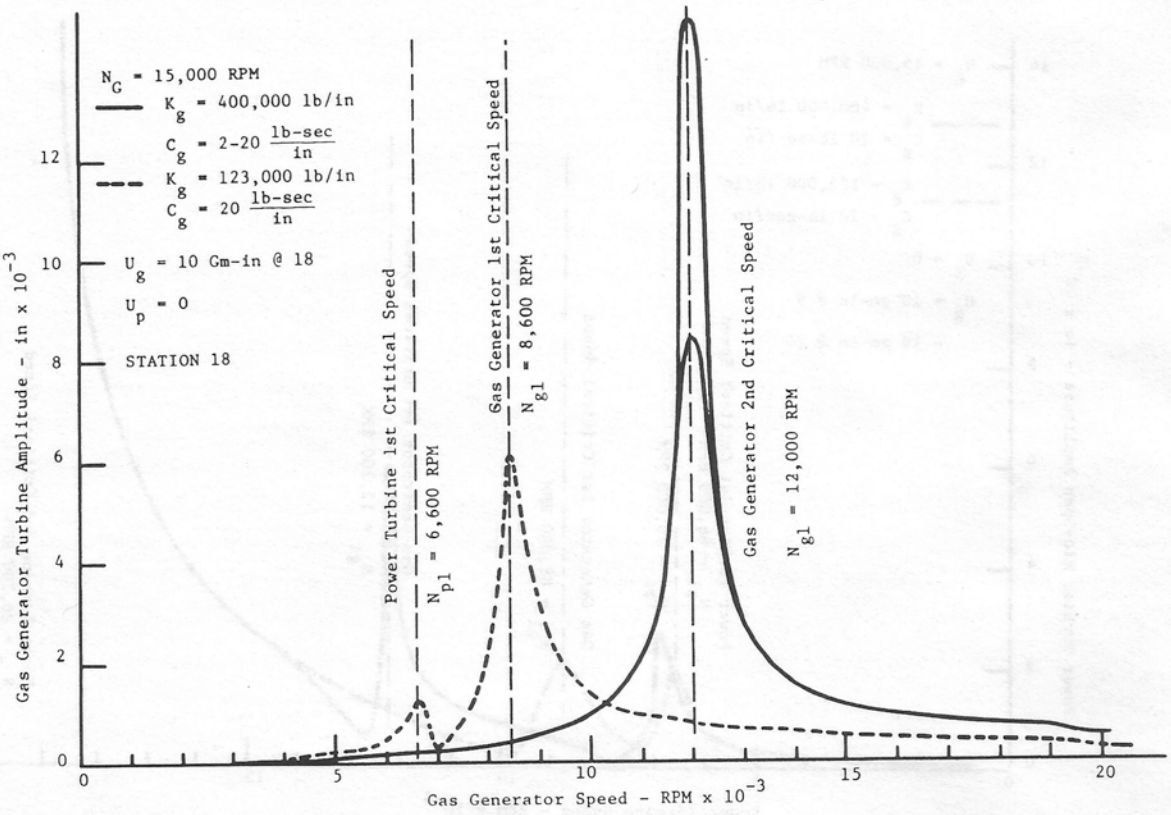

Fig. 14 Gas Generator Turbine Amplitude Due to Gas Generator Turbine Unbalance

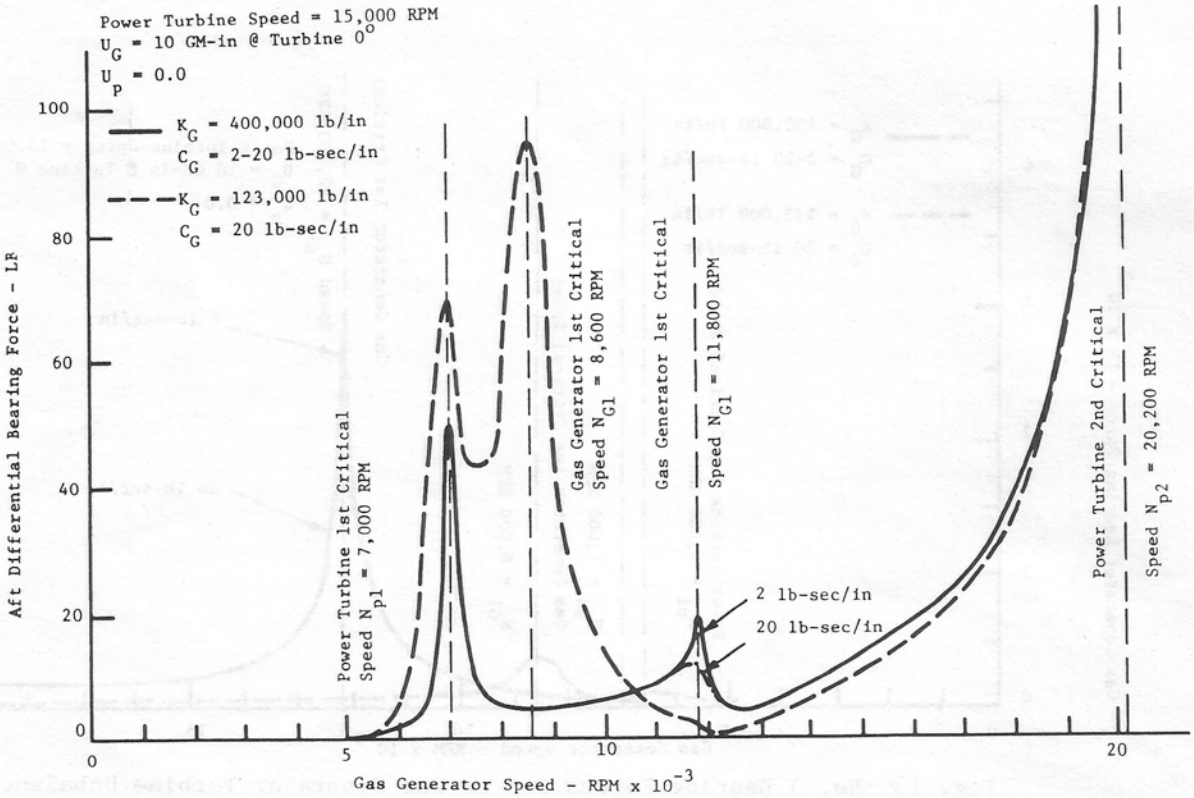

Fig. 15 Aft Intershaft Differential Bearing Load Due to Gas Generator Turbine Unbalance

TABLE 1

Bearing Loads Due to Gyroscopic Moments
Induced by Helicopter Yaw Motion

STATION NUMBER	DESCRIPTION	EFFECTS DUE TO GAS GENERATOR GYROSCOPIC FORCES		EFFECTS DUE TO POWER TURBINE GYROSCOPIC FORCES	
		AMPLITUDE in x 10^{-3}	FORCE lb.	AMPLITUDE in x 10^{-3}	FORCE lb.
5	Fwd Bearing	_____	404	_____	16
13	Aft Bearing	_____	347	_____	669
15	G. G. #3 Brg.	_____	1163	_____	66
21	P. T. #4 Brg.	_____	40	_____	138
18	Gas Generator Turbine	2.38	_____	1.24	_____
19	Power Turbine	0.16	_____	2.19	_____
18	Turbine Seal	1.69	_____	4.4	_____

Yaw Rate = 0.0033 RPM, N_g = 17,400 RPM, N_p = 17,400 RPM

occur at the No. 3 and aft intershaft bearing locations. The load on the aft intershaft differential bearing of 669 lb due to power turbine rotor gyroscopics is very close to the load for an L10 life of 500 hours for that bearing. The amplitudes of vibration at the turbine sections are relatively small.

The unbalance response studies indicate that the design of the No. 3 bearing on the gas generator rotor strongly affects the engine response and aft intershaft differential bearing forces. A squeeze film bearing applied at that location must be carefully designed to insure adequate engine performance.

NONLINEAR RESPONSE WITH SQUEEZE FILM BEARING

Because of the high bearing loads that can be transmitted through the No. 3 bearing and the supporting structure due to gas generator turbine unbalance, a squeeze film damper was incorporated behind the No. 3 bearing. The squeeze film damper consists of an 0.004 in. radial clearance space around the outer race of the No. 3 bearing with oil supplied to the annular region. In the original design, a retainer spring connecting the outer race of the bearing to the supporting diaphram structure was not used. Unbalance in the gas generator turbine will cause a precessive journal motion in the oil film which will in turn generate a hydrodynamic force in the oil film, producing an equivalent stiffness and damping effect. The forces and motion of the system are highly complex and are functions of both the static and dynamic journal loading. The oil film was modeled using the short bearing approximation to Reynolds equation (6) and was considered incompressible and isoviscous.

In its original configuration, the squeeze film bearing was 0.45 in. in length, with journal radius of 2.55 in. The oil viscosity was assumed to be 3.82×10^{-6} lb-s/in.^{2} Figure 16 illustrates the nonlinear limit cycles for the original bearing with the radial clearance ranging from 0.004 to 0.006 in. The dynamic unbalance loading is 66 gm-in. The unbalance parameter EMU is defined as e_u/c, where e_u is the equivalent mass eccentricity required to produce a given unbalance magnitude. The gas generator rotor speed was taken to be 16,800 RPM.

In Figs. 16a and 16b the effect of removing the journal preload centering or retainer spring is shown. In both cases the bearing is dynamically overloaded and the journal orbit nearly fills the available clearance. The dynamic force transmitted to the bearing and support structure is approximately 6.2 times the dynamic unbalance force in each case (TRD = 6.2). In Fig. 16c, the radial clearance has been increased to 0.006 in., thus reducing EMU. The dynamic force transmissibility increased to TRD = 7.14. Thus, a dynamic load of 8,433 lb is transmitted to the bearing housing. In Fig. 16d, the oil supply pressure was increased to 400 psi above the assumed fluid cavitation pressure to reduce the radial hydrodynamic forces on the squeeze bearing journal. The effects are similar to the previous cases. The large amplitude limit cycle orbits of Fig. 16 are indicative of a dynamically overloaded system.

To increase the dynamic load capacity of the squeeze film bearing,

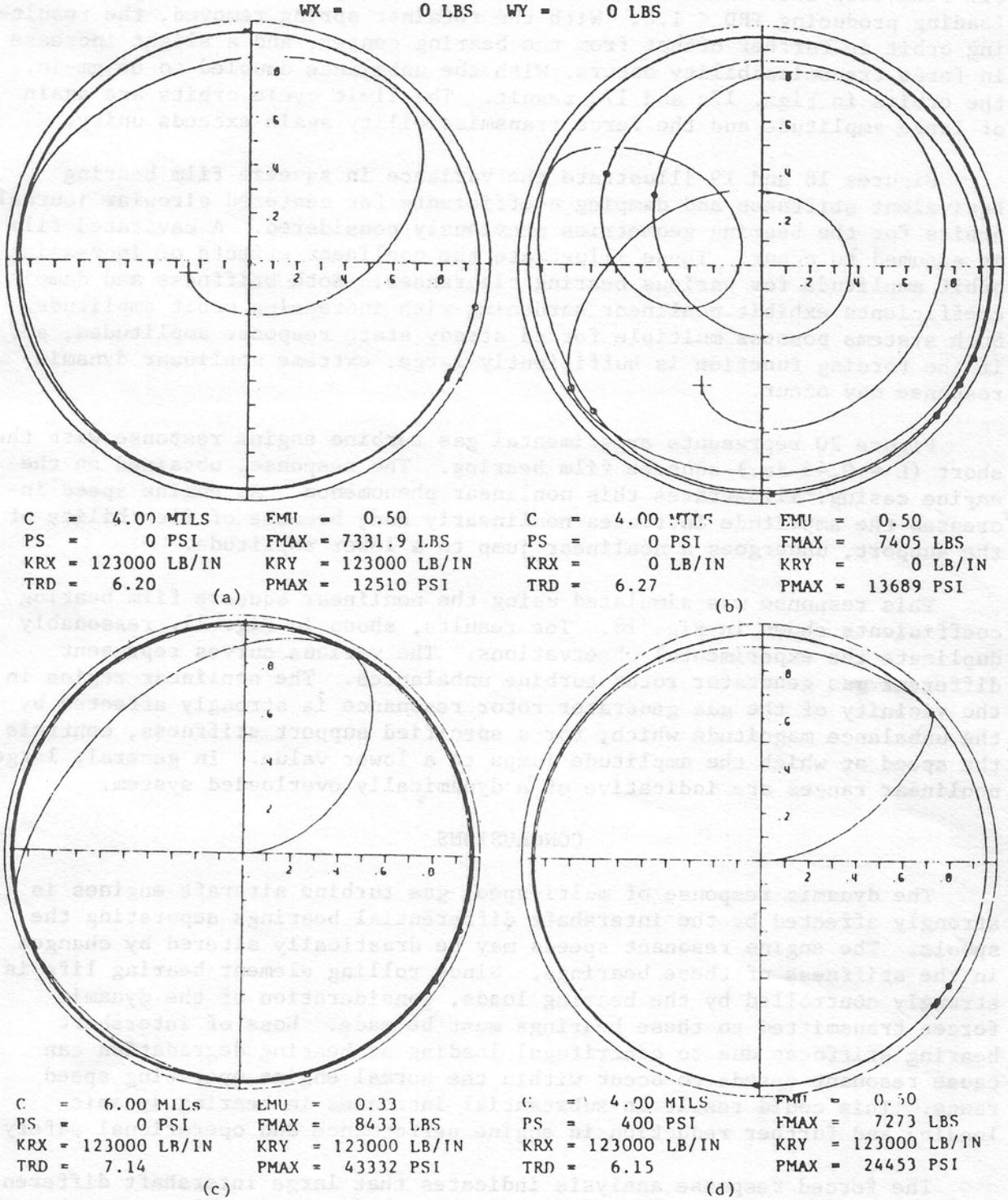

Fig. 16 Transient Motion of No. 3 Bearing Squeeze Film Bearing, L = 0.45 in.

the bearing length was assumed doubled to 0.90 in. The resulting limit cycle orbits are shown in Fig. 17. In each case, the clearance was taken as 0.004 in. and the effect of removing the preload or retainer spring was examined. For a dynamic unbalance of 33 gm-in (EMU = 0.25) the limit cycles shown in Figs. 17a and 17b are of relatively small amplitude. The oil film both with and without the retainer spring attenuates the dynamic loading producing TRD < 1.0. With the retainer spring removed, the resulting orbit is further offset from the bearing center, and a slight increase in force transmissibility occurs. With the unbalance doubled to 66 gm-in., the orbits in Figs. 17c and 17d result. The limit cycle orbits are again of large amplitude and the force transmissibility again exceeds unity.

Figures 18 and 19 illustrate the variance in squeeze film bearing equivalent stiffness and damping coefficients for centered circular journal orbits for the bearing geometries previously considered. A cavitated film is assumed to occur. These illustrate the nonlinear effects of increasing orbit amplitude for various bearing clearances. Both stiffness and damping coefficients exhibit nonlinear hardening with increasing orbit amplitude. Such systems possess multiple forced steady state response amplitudes, and if the forcing function is sufficiently large, extreme nonlinear dynamic response may occur.

Figure 20 represents experimental gas turbine engine response with the short (L = 0.45 in.) squeeze film bearing. The response, obtained on the engine casing, illustrates this nonlinear phenomenon. As engine speed increases the amplitude increases nonlinearly and, because of flexibility of the support, undergoes a nonlinear jump to a lower amplitude.

This response was simulated using the nonlinear squeeze film bearing coefficients shown in Fig. 18. The results, shown in Fig. 21, reasonably duplicate the experimental observations. The various curves represent different gas generator rotor turbine unbalances. The nonlinear region in the vicinity of the gas generator rotor resonance is strongly affected by the unbalance magnitude which, for a specified support stiffness, controls the speed at which the amplitude jumps to a lower value. In general, large nonlinear ranges are indicative of a dynamically overloaded system.

CONCLUSIONS

The dynamic response of multi-spool gas turbine aircraft engines is strongly affected by the intershaft differential bearings separating the spools. The engine resonant speeds may be drastically altered by changes in the stiffness of these bearings. Since rolling element bearing life is strongly controlled by the bearing loads, consideration of the dynamic forces transmitted to these bearings must be made. Loss of intershaft bearing stiffness due to centrifugal loading or bearing degradation can cause resonant speeds to occur within the normal engine operating speed range. This could result in substantial increases in bearing dynamic loading and further reduction in engine performance and operational safety.

The forced response analysis indicates that large intershaft differential bearing dynamic loading can occur even when operational speeds are not coincident with engine resonant speeds. Furthermore, these forces are

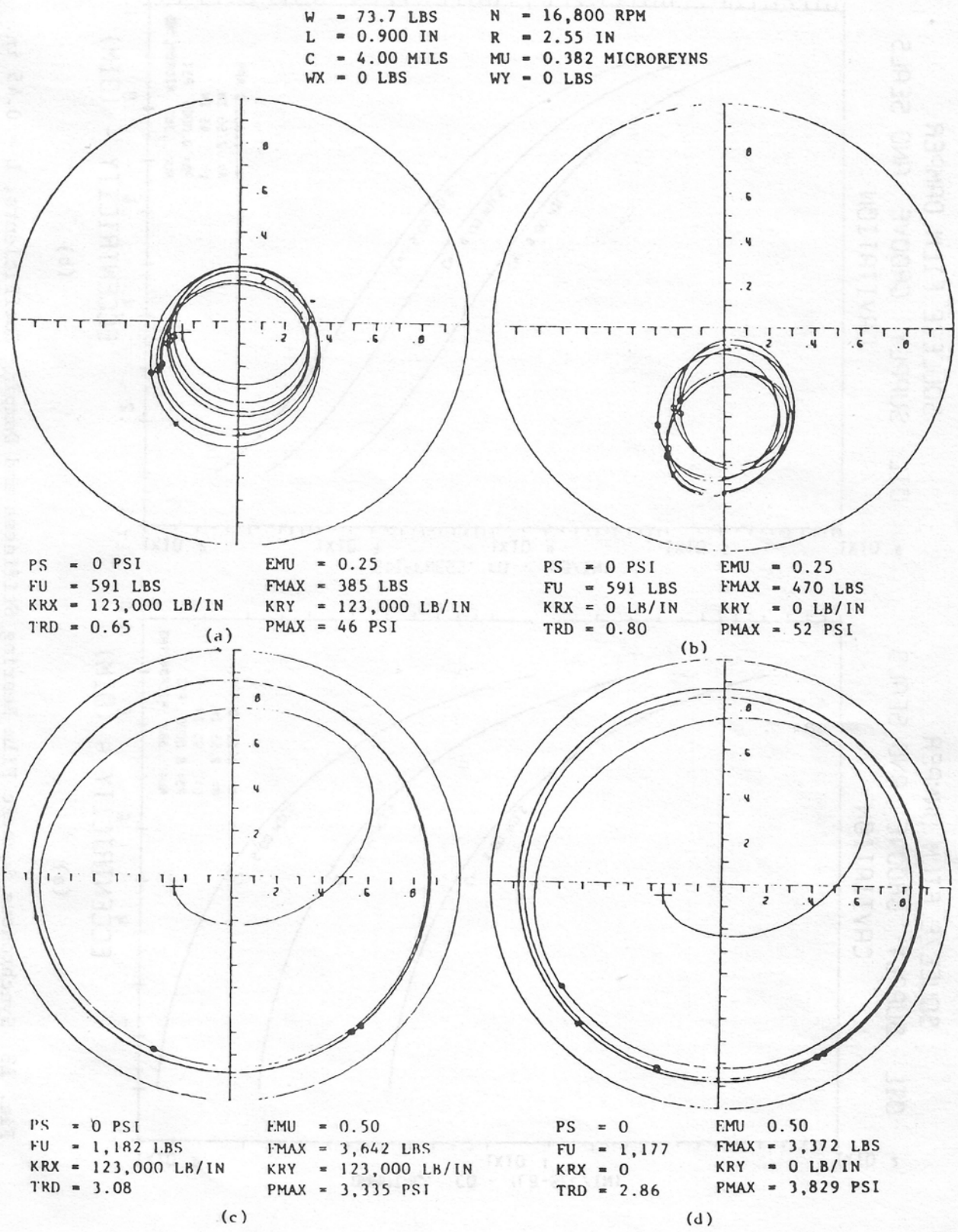

Fig. 17 Transient Motion of No. 3 Bearing Squeeze Film Bearing, L = 0.90 in.

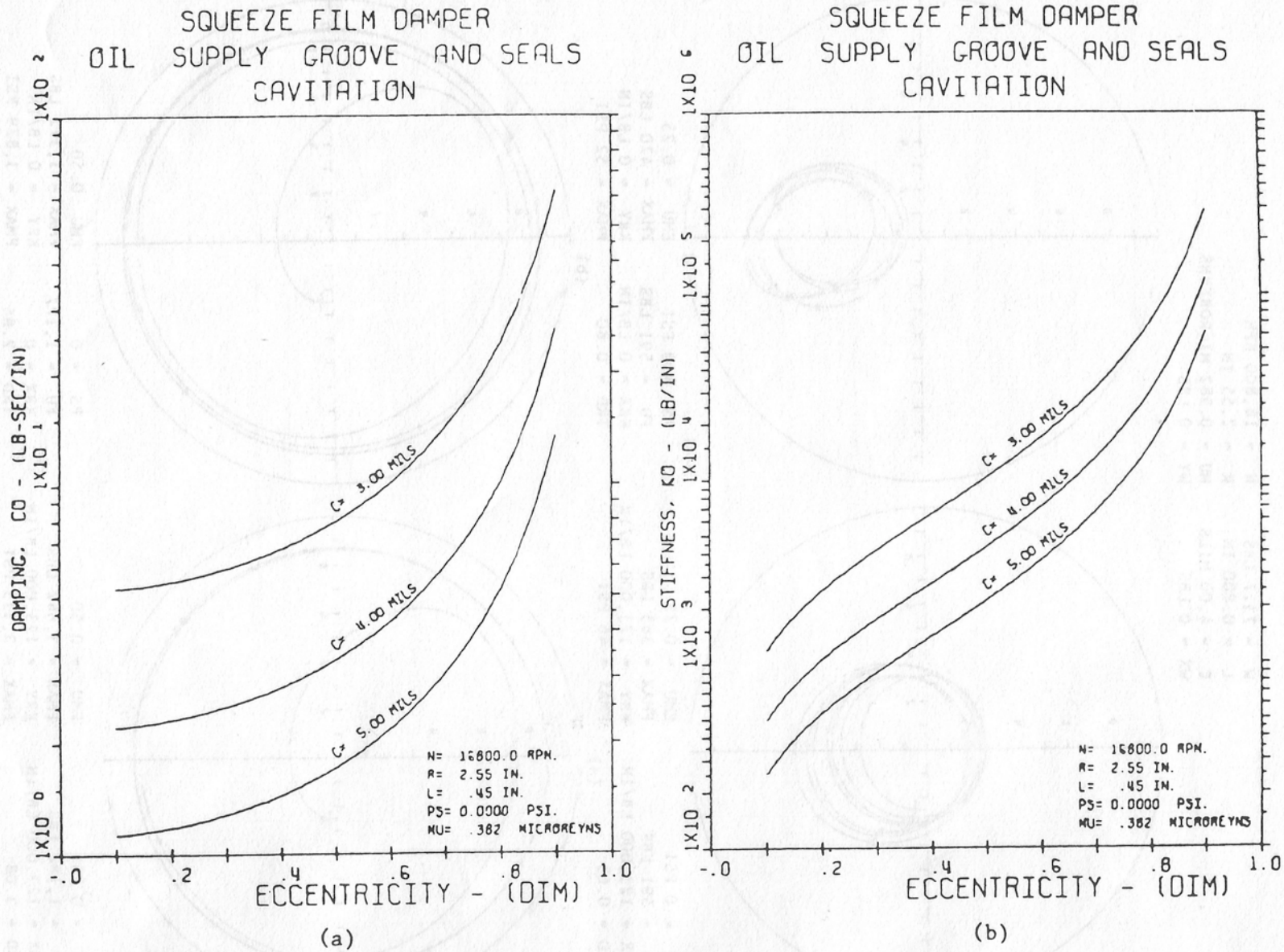

Fig. 18 Synchronous Squeeze Film Bearing Stiffness and Damping Coefficients, L = 0.45 in.

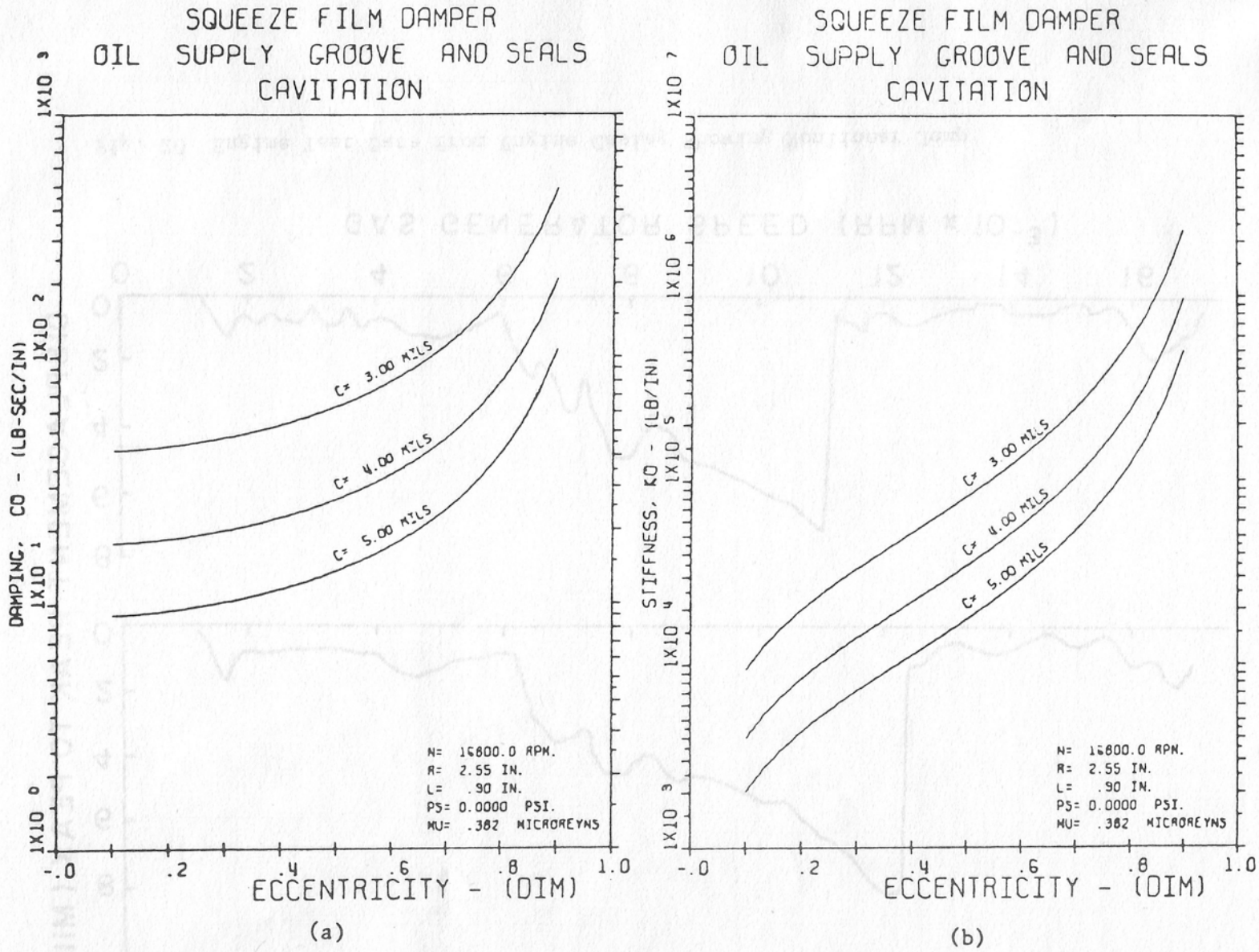

Fig. 19 Synchronous Squeeze Film Bearing Stiffness and Damping Coefficients, L = 0.90 in.

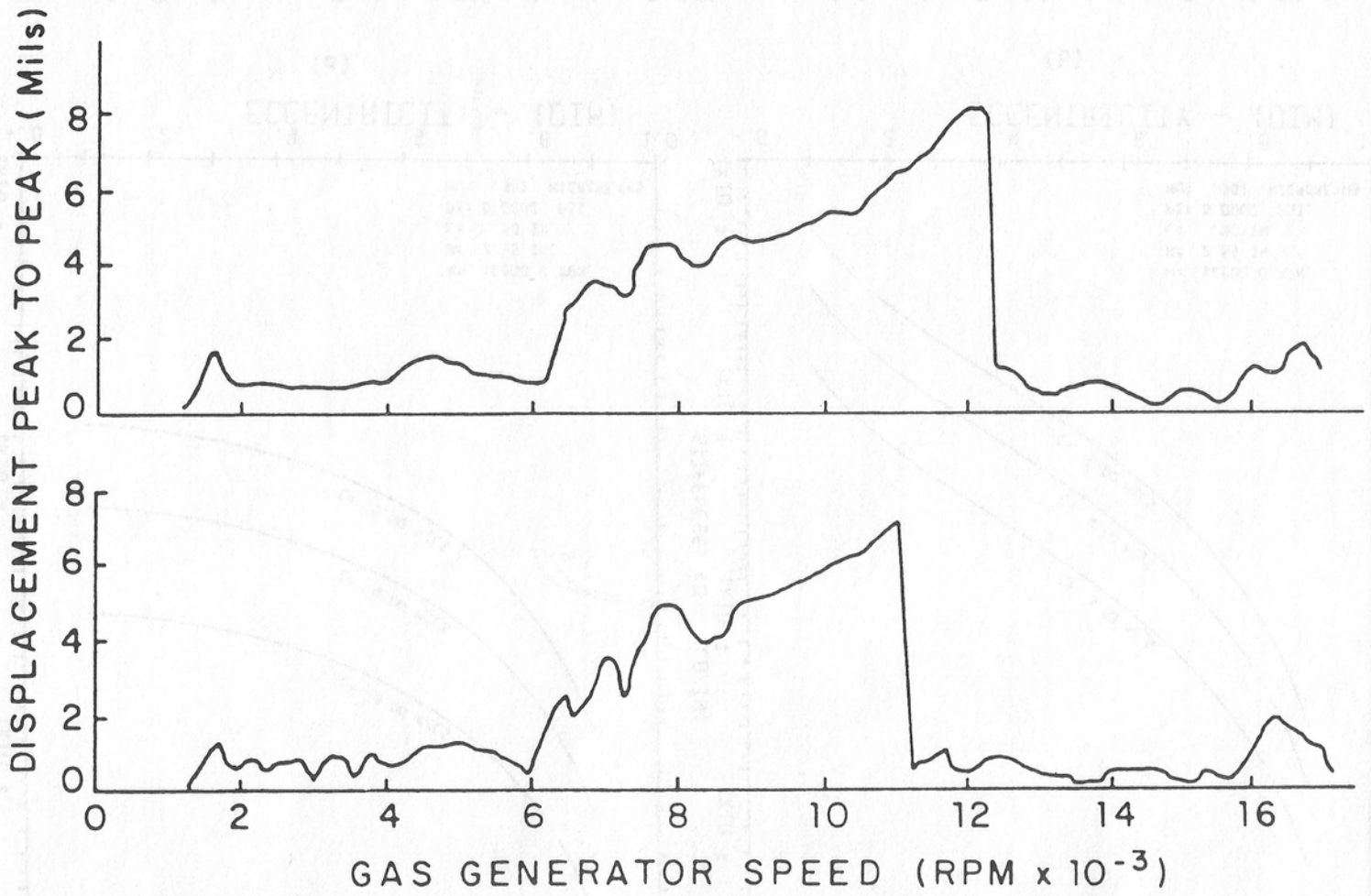

Fig. 20 Engine Test Data from Engine Casing Showing Nonlinear Jump

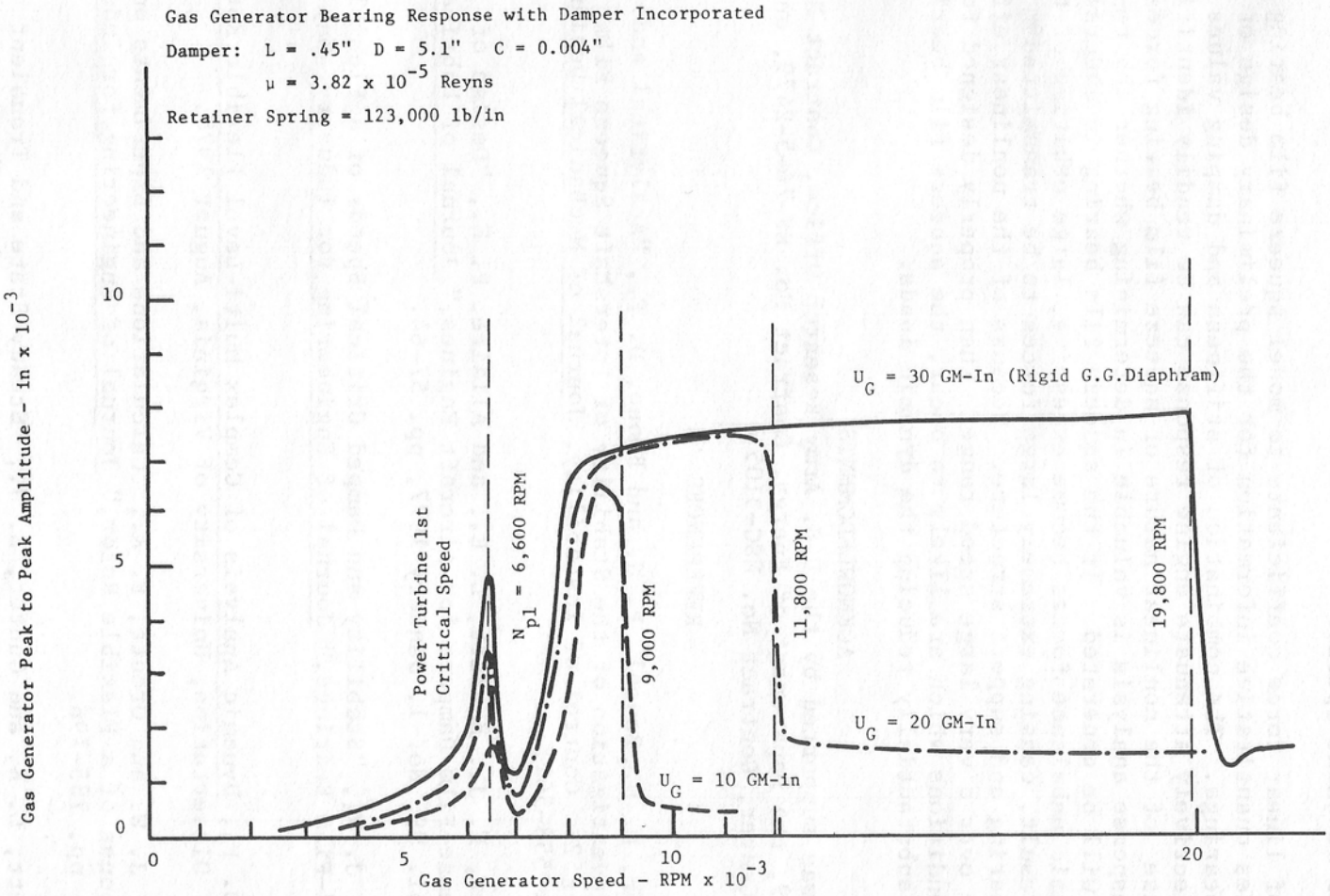

Fig. 21 Gas Generator Rotor Bearing Amplitudes with Nonlinear Squeeze Film Bearing Simulation Showing Nonlinear Amplitude Jump

strongly affected by the location and magnitude of viscous damping mechanisms in the system. It is apparent that with highly flexible rotor systems, viscous damping at a single location will not necessarily suppress resonant response at all resonant speeds.

The use of linear force coefficients to model squeeze film bearing effects provides quantitative information for the preliminary design of squeeze film bearings. The combination of stiffness and damping values which will effectively attenuate engine response can be readily identified. However, because of the nonlinear nature of squeeze film bearing forces, a nonlinear response analysis is valuable in determining whether the required forces will be generated. If the squeeze film bearing is undersized or if the dynamic unbalance forces become excessive, large orbiting of the journal will result, causing extremely large forces to be transmitted through the bearing and support structure. Because of the nonlinear effects, this may occur over a very large speed range. When properly designed for the dynamic conditions which are likely to occur, the squeeze film bearing is capable of substantially reducing the dynamic loads.

ACKNOWLEDGMENTS

This work was supported by the U.S. Army Research Office, Contract No. DAG 29-77C-0009, the Department of Energy, Contract No. EF-76-5-2479, and NASA Research Center, Contract No. NSG-3105

REFERENCES

1. Hibner, D. H., Bansal, P. N. and Buono, D. F., "Analytical and Experimental Investigation of the Stability of Intershaft Squeeze Film Bearings - Part 2: Control of Instability, Journal of Mechanical Design, July 1978, pp. 558-562.

2. Gunter, E. J., Barrett, L. E., and Allaire, P. E., "Design of Nonlinear Squeeze-Film Dampers for Aircraft Engines," Journal of Lubrication Technology, Vol. 99, No. 1, January 1977, pp. 57-64.

3. Lund, J. W., "Stability and Damped Critical Speeds of a Flexible Rotor in Fluid-Film Bearings," Journal of Engineering for Industry, May 1974, pp. 509-517.

4. Li, D. F., Dynamic Analysis of Complex Multi-Level Flexible Rotor Systems, Ph.D. Dissertation, University of Virginia, August 1978.

5. Lund, J. W. and Orcutt, F. K., "Calculations and Experiments on the Unbalance Response of a Flexible Rotor," Journal of Engineering for Industry, November 1967, pp. 785-796.

6. Barrett, L. E. and Gunter, E. J., "Steady State and Transient Analysis of a Squeeze Film Bearing for Rotor Stability," NASA CR-2548, May 1975.

DISCUSSION

D. L. Taylor, Assistant Professor, Sibley School of Mechanical & Aerospace Engineering, Cornell University.

Since many of the questions and comments during the workshop dealt with the phenomenon of bistable operation, it is worthwhile pointing out some interesting aspects of this type of response. These comments are particularly relevant to the presentation of the work by Professor Gunter because they deal with a similar rotor system. When using numerical integration to analyze the transient response of squeeze film damper systems, a primary question which must be addressed is how long to integrate the solution in time. Many presentors at the workshop have shown computer generated orbits that appear to involve only three or four orbits, which is quite understandable in terms of computer expense. However, the discussor has found that some solutions which appear to be steady state are deceptive.

Consider a planar rigid rotor carried in a squeeze film isolator (damper and centering spring in parallel). The values of the parameters given in the following table are taken from Professor Gunter's paper (which it will be noted is <u>not</u> a single planar rotor). An Ocvirk short bearing π film is used for bearing forces. The differential equations can be obtained and integrated numerically. The planar model is found to display bistable operation over a speed range of approximately 10,000 rpm to 14,000 rpm. Several questions during the discussion dealt with methods of numerical integration. The results which follow are based on a variable time step Kutta-Merson algorithm. This type of program will constantly adjust the effective time step of the integrator to maintain a requested degree of accuracy. The discussor has found this type of algorithm to be very effective. It can handle quite rapid transients such as blade loss but tracks an almost circular orbit with approximately six to ten time steps per revolution. This is quite efficient with regards to computer time. The orbits which follow were generated by such an algorithm using a requested time step of .00032 sec. The plots appear to be crude simply because of the large time steps involved. The sharp corners result from the plotting program which connects the calculated points with straight lines. Much smaller time steps (100 or 1,000 times smaller) lead to orbits which still pass through the points which are plotted (the corners).

Any transient solution must begin from specific initial conditions. The orbit in Figure 1 shows the orbit calculated for initial conditions of initial eccentricity of 1. mil, initial eccentric velocity of 0., initial whirl velocity of 12,000 rpm (synchronous) and initial phase relationship between shaft center displacement and mass center displacement of .7 radians. The orbit starts from the circled point, settles into a radius of 3.09 mils, but later diverges from this orbit and finally settles into a whirl orbit of about 1.8 mils. The true nature of the response is better understood from Figure 2 which shows the eccentricity plotted versus time.

The pitfall to beware in numerical integration can be seen from Figure 2 where it is very tempting to stop the integration at about t = .05 sec. This phenomenon has not been completely understood by the discussor but has been observed many times. The major pattern is that it always involved initial convergence to the higher of the two possible orbits. Also, even though the eccentricity appears to be relatively constant for a long period in Figure 2, the phase angle between the shaft center and the mass center is steadily shifting. The question raised concerns its observance by other investigators (experimentally or computationally).

Table 1

m =	73.8 lb	Ω =	12,000 rpm
k =	1.23×10^6 lb/in	R =	2.55 in
μ =	.0266 poise	L =	.9 in
d =	1 mil (c.g. offset)	C =	4 mil

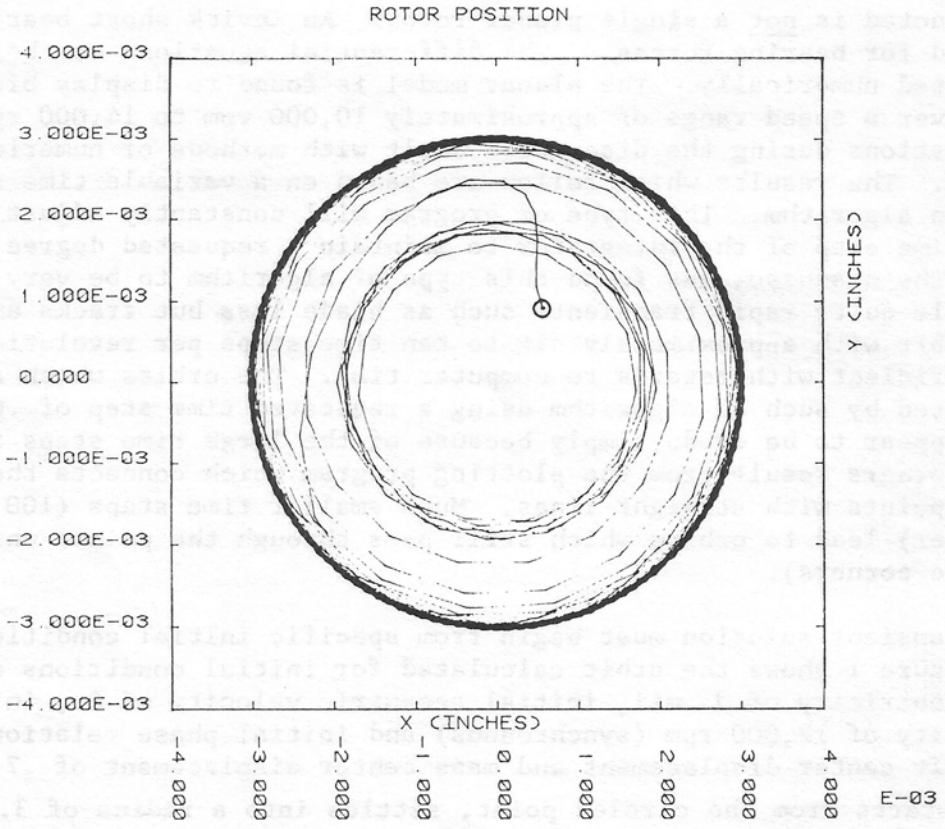

Fig. 1 Transient whirl orbit, x-y location of shaft center

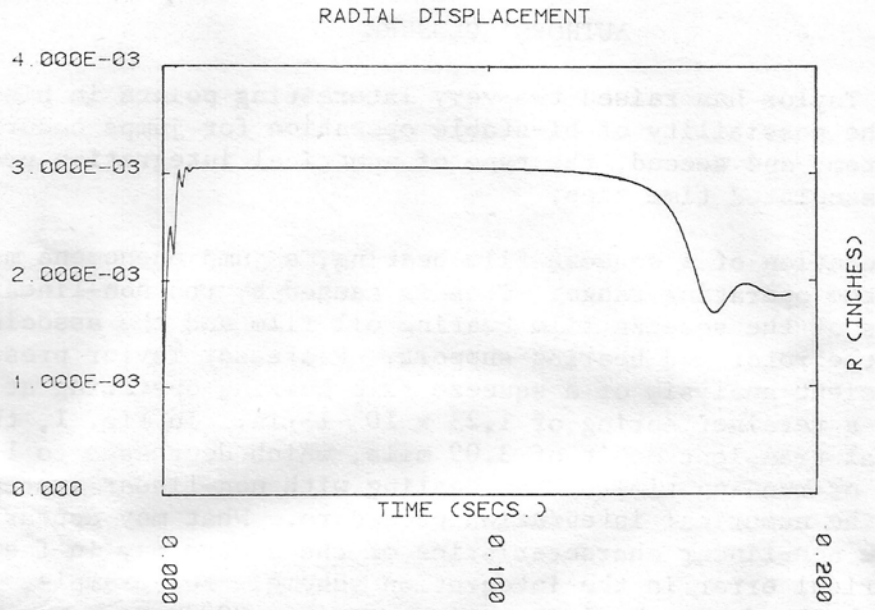

Fig. 2 Transient eccentricity versus time

AUTHORS' CLOSURE

Professor Taylor has raised two very interesting points in his discussion. First, the possibility of bi-stable operation for jumps occurring in a non-linear system, and second, the type of numerical integration procedure used and the associated time step.

In the operation of a squeeze film bearing, a jump phenomena may occur over parts of the operating range. This is caused by the non-linear characteristics of the squeeze film bearing oil film and the associated elasticity of the rotor and bearing support. Professor Taylor presents a numerical transient analysis of a squeeze film bearing operating at 12,000 rpm, including a retainer spring of 1.23×10^6 lb/in. In Fig. 1, the orbit shows an initial transient orbit of 3.09 mils, which decreases to 1.8 mils after .15 sec. of running time. When dealing with non-linear systems, one must evaluate the numerical integration procedure. What may appear to be a jump due to the non-linear characteristics of the system may in fact be caused by numerical error in the integration scheme. For example, in the procedure used by Professor Taylor, a time step of .00032 sec. was used. At an operating speed of 12,000 rpm, this is equivalent to only 15.6 steps per cycle. To accurately determine whether this non-linear jump is truly occurring, the integrated solution should be run with a much finer time step. Professor Taylor mentioned that although the eccentricity appears to be relatively constant for a long period, as shown in Fig. 2, the phase angle between the shaft center and the mass center is steadily shifting. This has been observed in a number of instances and has been associated with the numerical propagation of error in the solution.

PROCEEDINGS

OF THE

CONFERENCE ON THE STABILITY AND DYNAMIC RESPONSE OF ROTORS WITH SQUEEZE FILM BEARINGS

8-10 MAY 1979

U. S. ARMY RESEARCH OFFICE
RESEARCH TRIANGLE PARK, NORTH CAROLINA

APPLIED TECHNOLOGY LABORATORY
U.S. ARMY RESEARCH AND TECHNOLOGY LABORATORIES (AVRADCOM)
FORT EUSTIS, VIRGINIA